Available online at www.sciencedirect.com
ScienceDirect
Journal of Catalysis 242 (2006) 278–286
JOURNAL OF CATALYSIS
www.elsevier.com/locate/jcat

A comparison of the esterification of acetic acid with methanol using heterogeneous versus homogeneous acid catalysis

Yijun Liu, Edgar Lotero, James G. Goodwin Jr. *

Department of Chemical and Biomolecular Engineering, Clemson University, Clemson, SC 29634, USA

Received 27 March 2006; revised 4 May 2006; accepted 20 May 2006

Available online 18 July 2006

Abstract

To investigate the similarities and differences between heterogeneous and homogeneous catalyzed esterification, the kinetics of acetic acid esterification with methanol were investigated using a commercial Nafion/silica nanocomposite catalyst (SAC-13) and H_2SO_4, respectively. Reactions were carried out in an isothermal well-mixed batch reactor at 60 °C. Organic base titration, TGA, and elemental sulfur analysis were carried out to estimate the acid site density of SAC-13, permitting the assessment of its catalytic performance for esterification on a per site basis. It was found that SAC-13 has comparable site activity for acetic acid esterification as H_2SO_4. SAC-13 and H_2SO_4 also exhibited similar reaction inhibition due to the presence of water. The similar response to the presence of water and the results of pyridine poisoning experiments suggest that esterification with these catalysts occurs through a common reaction mechanism. Consistent with the hypothesized homogeneous-type reaction mechanism, reaction on SAC-13 appears to involve single-site catalysis with a probable rate-controlling Eley-Rideal surface reaction. A mechanistically derived kinetic model successfully predicts the esterification rate of SAC-13 as reaction progresses. The dissimilarities between homogeneous and heterogeneous acid-catalyzed esterification are also discussed.

Keywords: Acetic acid esterification; Sulfuric acid; Nafion/silica (SAC-13); Heterogeneous vs homogeneous mechanism

1. Introduction

Organic esters are important fine chemicals used widely in the manufacturing of flavors, pharmaceuticals, plasticizers, and polymerization monomers. They are also used as emulsifiers in the food and cosmetic industries. Several synthetic routes are available for obtaining organic esters, most of which have been briefly reviewed by Yadav and Mehta [1]. The most-used methodology for ester synthesis is direct esterification of carboxylic acids with alcohols in the presence of acid catalysts.

Strong liquid mineral acids, such as H_2SO_4, HCl, and HI, are effective for the esterification of carboxylic acids. These homogeneous acid catalysts and others have been the subjects of extensive studies. For instance, it has been well documented that when using this type of catalyst, the slow step of the reaction is the nucleophilic attack of the alcohol on the protonated carbonyl group of the carboxylic acid [2,3]. This mechanistic route first involves protonation of the carboxylic acid, which activates it for reaction with nonprotonated methanol to yield a tetrahedral intermediate that, by decomposition, produces the products of reaction, ester and water.

On solid acid catalysts with mainly Brønsted acid sites, one might expect a similar esterification behavior with a homogeneous-like mechanism mediating the molecular transformation [4]. However, thus far, there appears to be no consensus about the reaction mechanism occurring on different (although similar) solid acid catalysts. In particular, the literature contains many contradictory reports about whether esterification occurs via a single-site (Eley-Rideal [E-R]) or a dual-site mechanism. For instance, using kinetic correlations of experimental data, Teo and Saha [5] and Lee et al. [6] found that a dual-site model better fit the behavior of acid resin catalysts used in the esterification of acetic acid with amyl alcohol. In contrast, for the esterification of hexanoic acid with 1-octanol using zeolite BEA and SAC-13, an E-R kinetic model yielded better results, with 15% less error in fitting the experimental

* Corresponding author. Fax: +1 864 656 0784.
E-mail address: james.goodwin@ces.clemson.edu (J.G. Goodwin Jr.).

0021-9517/$ – see front matter
doi:10.1016/j.jcat.2006.05.026

reaction results [7]. Altiokka and Citak [8] proposed an E-R mechanism involving the reaction of isobutanol adsorbed on the acid sites of an Amberlyst catalyst with free acetic acid from the bulk solution as the primary route for esterification. However, just the opposite picture was proposed by Lilja et al. [9], who suggested the rate-determining reaction step to be the nucleophilic attack by liquid alcohol on the adsorbed carboxylic acid on the Brønsted acid sites of Amberlyst-15.

The focus of the present study was to provide a fundamental insight into the similarities and differences existing between heterogeneous and homogeneous Brønsted acid-catalyzed esterification. Here esterification on a solid acid catalyst, SAC-13 (Nafion resin supported on a porous silica matrix), was compared with esterification in the presence of H_2SO_4. The resin/silica composite is strongly acidic, with highly accessible sites and sufficient robustness to withstand reasonably high temperatures (∼200 °C) and attrition stress [10]. When only protons are available as active acid sites similar to H_2SO_4, one might expect SAC-13 to exhibit catalytic behavior resembling that of the homogeneous catalyst. Thus, the similarity between these two catalysts provides a good way to examine the effect of the heterogeneous catalyst surface on catalyst activity and mechanistic pathway. Determination of reaction kinetic parameters together with the derivation of an analytical kinetic model able to satisfactorily explain our experimental observations led to some important insights. The derived kinetic model was also able to account for the apparent contradictory reports from other authors on esterification catalyzed by solid acids.

2. Experimental

Methanol (MeOH, 99.9 wt%, Acros Organics), acetic acid (Hac, 99.7 wt%, Aldrich), and tetrahydrofuran (THF, 99.9 wt%, Aldrich) were used without further purification. Concentrated sulfuric acid was purchased from Fisher Scientific, and SAC-13 was obtained from Aldrich. SAC-13 was dehydrated at 80 °C under vacuum and stored in a desiccator until use.

Thermogravimetric analysis was conducted using a Perkin–Elmer Pyris 1 instrument to determine the Nafion loading on the composite catalyst. Under a nitrogen atmosphere, the temperature was first stabilized at 25 °C for 30 min and then ramped to 700 °C at a rate of 10 °C/min. The fraction of Nafion in the composite was calculated based on the weight loss observed in the range 280–500 °C, corresponding to the decomposition window for Nafion-H domains [10]. Elemental sulfur analysis of SAC-13 was performed by Galbraith Laboratories. Pyridine adsorption experiments were carried out by saturating SAC-13 in a solution containing a known concentration of pyridine in THF. Gas chromatography was used to quantify the amount of pyridine adsorbed on the catalyst, calculated from the difference in pyridine concentration in solution before and after SAC-13 saturation.

Reactions were carried out in an isothermal well-stirred batch reactor as described previously [11]. In brief, before the reaction, reagent mixtures (methanol and acetic acid in a 2:1 molar ratio, as well as the solvent THF) were heated to the desired temperature while being continuously stirred. Once the desired temperature was reached, the esterification reaction was started by charging the catalyst.

For the pure resin catalyst (Nafion), swelling of the polymer network in polar solvent is known to occur. However, for SAC-13 (Nafion/silica), only negligible swelling has been reported [12] due to the high dispersion of the polymeric domain on the high-surface area SiO_2. However, even slight catalyst swelling could affect catalytic activity because during swelling, additional acid sites can be exposed, falsifying kinetic measurements. To assess whether swelling played a role in catalyst activity, SAC-13 was presoaked in polar MeOH overnight before the reaction, and esterification was then initiated by charging the acetic acid and THF, which are known to have much less capability to swell the polymeric resin in SAC-13 than methanol [13]. Under these conditions, identical reaction profiles were obtained as in experiments using the catalyst charged last. This confirms that catalyst swelling due to methanol had a negligible effect on the reaction rate.

A SAC-13 loading of 1.09 g/45 ml in its pellet form (1 mm), as provided by the vendor, and a stirring rate of 1133 rpm were used in all reaction experiments. Diffusional limitations were ruled out by varying the particle size and stirring rate between 0.10–1 mm and 850–1700 rpm, respectively. No change in reaction rate was detected when using particles smaller than 1 mm or stirring speeds above 850 rpm. A microscale syringe was used for sampling at definite time intervals. Sample analysis using a Hewlett–Packard 6890 gas chromatograph followed the same procedure as used in previous work [11].

Plots of acetic acid conversion (X_A) versus reaction time (t) were linear at conversions <10% for both liquid and solid acid catalysts (Fig. 1). Despite the fact that second-order kinetics are well documented for H_2SO_4, this linearity observation is expected due to the use of a high substrate-to-catalyst ratio (>1200) [14]. In this way, the concentration of protonated complex changed only negligibly at low conversion (<10%). Thus, values for initial reaction rates were calculated as $r = C_{A,0}(dX_A/dt)$, where $C_{A,0}$ is the initial concentration of the carboxylic acid and X_A is the conversion of the carboxylic acid.

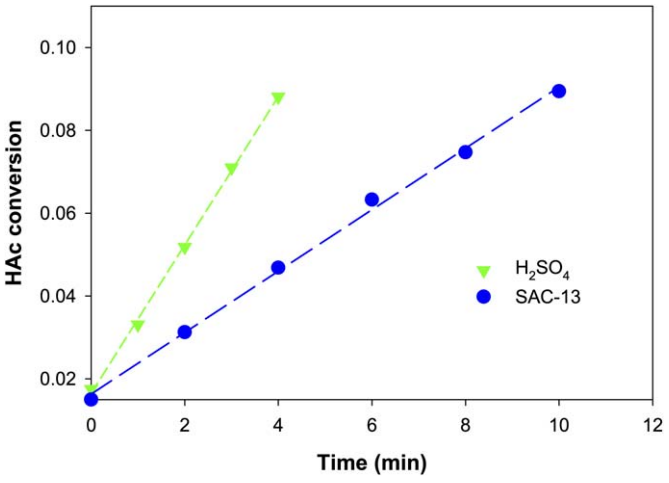

Fig. 1. Initial reaction period for esterification of acetic acid with methanol at 60 °C using (▼) H_2SO_4 (0.011 g/45 ml) and (●) SAC-13 (1.09 g/45 ml).

In addition, despite the catalytic activity of acetic acid itself [11,15], the autocatalysis could be ignored under the present experimental conditions because of its negligible contribution to the overall reaction rate.

3. Results

3.1. Acid site density characterization

The maximum expected acid site density of SAC-13 can be estimated by TGA or sulfur element analysis [10,16], because each sulfonic acid group constitutes a potential acid site. TGA analysis (not shown) yielded an average of 14.5 wt% Nafion loading on the silica matrix, corresponding to an acid site density of 0.129 mmol/g. This agrees well with the value of 0.131 mmol/g determined from elemental sulfur analysis carried out by the Galbraith Laboratory using ICP. Liquid-phase pyridine adsorption experiments can also be used for surface acid site density determination (Table 1). Nevertheless, organic base adsorption on the silanol groups of silica matrix must be excluded. Pyridine adsorption experiments with sodium-exchanged SAC-13 ($NaO–SO_2/SiO_2$), obtained using aqueous NaCl solution as the ion-exchange reagent, showed that approximately 10% of the pyridine could be adsorbed on the silica matrix (Table 1). After adjustment, the acid site density of SAC-13 obtained from pyridine adsorption was about 0.129 mmol/g, conforming to the values calculated by TGA and elemental sulfur analysis.

3.2. Catalytic activity of H_2SO_4 and SAC-13

Fig. 2 compares the reactivity of acetic acid esterification at 60 °C catalyzed by sulfuric acid and SAC-13, respectively. On a per weight basis, the homogeneous acid catalyst was more active than the heterogeneous catalyst. Using a very small amount of H_2SO_4 (0.011 g/45 ml), acetic acid conversion reached 82% after 11 h of reaction time at 60 °C with 2× stoichiometric methanol. On the other hand, a hundredfold greater amount of SAC-13 (1.09 g/45 ml) was required to yield a similar reaction profile with 75% transformation of acetic acid after 11 h. The better catalytic activity of H_2SO_4 can be attributed to its greater density of acid sites per gram. Calculation of turnover frequencies (TOFs) provides a comprehensive way to make catalyst comparisons on a per site basis. Using the acid site density of 0.13 mmol/g for SAC-13 and assuming 1 mol H^+/1 mol H_2SO_4 by neglecting dissociation of the weak acid HSO_4^-, initial TOF values were calculated; these are given in Table 2. On a per site basis, the catalytic activity of H_2SO_4 was greater than that of SAC-13 by only a factor of 3.

Table 1
Pyridine adsorption on SAC-13 and Na^+-SAC-13

Catalyst	Solvent	T	Acid site density (mmol/g)[a]
SAC-13	THF	RT (25 °C)	0.143
SAC-13	THF	50 °C	0.145
Na^+-SAC-13	THF	RT	0.016

[a] Experimental error: ±5%.

3.3. Effect of reactant composition on SAC-13 catalysis

Homogeneous acid-catalyzed esterification follows second-order kinetics, first-order with respect to each reagent [15,17]. The calculation of kinetic parameters for heterogeneous acid catalysts is complicated because of the complex catalyst surface-adsorbate interactions. As is typically done, apparent kinetic parameters, such as reaction orders, were determined by varying the concentration of one reactant while fixing that of the other at 2.0 M and measuring initial kinetics at 60 °C. The

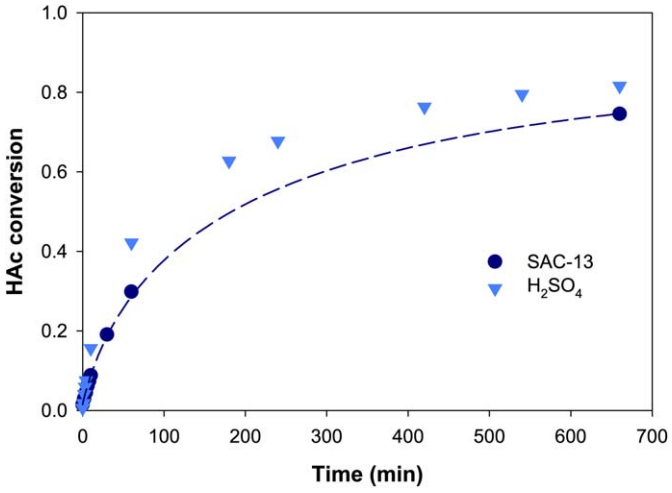

Fig. 2. Conversion vs time for acetic acid esterification catalyzed by (▼) H_2SO_4 (2.5 mM) and (●) SAC-13 (1.09 g/45 ml) at 60 °C ($C_{A,0} = 3$ M, $C_{M,0} = 6$ M, symbols represent the experimental data; dashed line represents the model prediction for SAC-13 catalysis).

Table 2
Initial kinetic parameter comparison for H_2SO_4 and SAC-13 catalyzed acetic acid esterification with MeOH at 60 °C ($C_{A,0} = 3$ M, $C_{M,0} = 6$ M)[a]

$C_{W,0}$ (M)[a]	H_2SO_4[b]			SAC-13[b]		
	TOF[c] (min^{-1})	E_a (kJ)	$(E_{a,h} - E_{a,l})$[e] (kJ)	TOF[d] (min^{-1})	E_a (kJ)	$(E_{a,h} - E_{a,l})$[e] (kJ)
0	22.76	52.7	11.1	7.28	51.8	10.4
2.85	3.07	63.8		1.66	62.2	

[a] $C_{A,0}$, $C_{M,0}$, and $C_{W,0}$ represent the initial concentrations of acetic acid, methanol, and water, respectively.
[b] Experimental error ±6%.
[c] 1 mol H^+/1 mol H_2SO_4 is assumed.
[d] The elemental analysis value for sulfur content of 0.131 mmol/g was used.
[e] The subscripts h and l represent high initial water concentration ($C_{W,0} = 2.85$ M) and low initial water concentration ($C_{W,0} = 0$ M), respectively.

Table 3
Initial reaction rate data for the determination of apparent reaction orders of methanol and acetic acid in SAC-13 (1.09 g/45 ml) catalyzed esterification at 60 °C

$C_{A,0}$ (M)	$C_{M,0}$ (M)	r_0[a] (M/min) × 10^3
2	2	8.05
2	4	13.3
2	6	17.0
2	14	25.6
4	2	13.9
5	2	15.7
6	2	18.4

[a] Experimental error ±6%.

results are given in Table 3. The concentrations of both alcohol and carboxylic acid had positive affects on the reaction rate with increasing reactant concentration. Using a power law approximation, the apparent reaction orders were determined to be 0.59 for methanol and 0.74 for acetic acid, with a correlation coefficient of 0.99–1.00.

3.4. Water sensitivity

In our previous work, the esterification byproduct water was found to significantly inhibit H_2SO_4 catalysis [11]. The resistance of solid catalysts to water poisoning is an important characteristic in determining their applicability for commercial esterification processes. The effect of water on acid-catalyzed esterification was studied using initial reaction kinetics (<10% conversion of the limiting reactant) with varying amounts of initially added water. This permits a better determination of the effect of water on the catalyst, because the rate is little affected by the reverse reaction when only small amounts of the methyl ester are present [11]. The concentrations of acetic acid and methanol were fixed at 3.0 and 6.0 M, respectively. Water addition experiments used THF (as a solvent), to keep the total reaction volume constant.

Fig. 3 shows acetic acid conversion on SAC-13 versus time at 60 °C for experiments using different initial concentrations of water ($C_{W,0}$). The catalytic activity was significantly inhibited with increasing water concentration in the reaction mixture. After 1 h of reaction, a reaction mixture with 2.85 M initial water concentration had a conversion about 60% lower than that with no initial water added. Chen et al. [18] have shown that when esterification is carried out using Nafion-H in the presence of an initial water concentration of 4.3 M, the conversion of acrylic acid after 4 h decreases from 60% without the addition of water to 30.6% at 80 °C. Hence, the response to water observed here for SAC-13 is consistent with what has been reported for the parent resin. Nevertheless, both SAC-13 and Nafion appear to be more resistant to water deactivation than other solid acids, such as SO_4^{2-}/ZrO_2 and Amberlyst-15 [18]. In particular, SO_4^{2-}/ZrO_2 is well known to suffer from serious leaching in media containing water [15,19].

In Fig. 4, the water sensitivities of SAC-13 and H_2SO_4 are compared using initial reaction rates. Here, activity ratios were used to put the results for the two catalysts on the same scale. C_W, the concentration of water, includes both the amount added

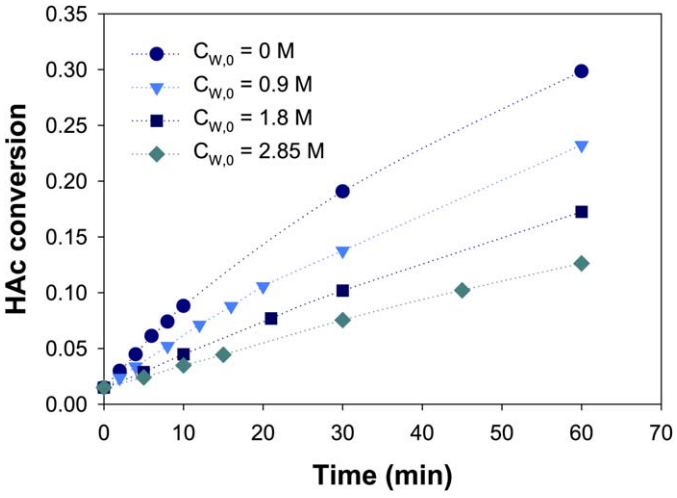

Fig. 3. Water sensitivity of acetic acid esterification catalyzed by SAC-13 at 60 °C.

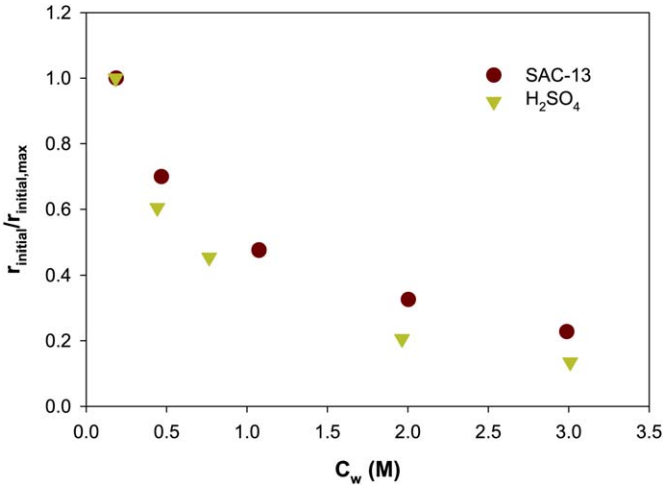

Fig. 4. Water sensitivity of acetic acid esterification with methanol at 60 °C ($C_{A,0}$ = 3 M, $C_{M,0}$ = 6 M) on (●) SAC-13 compared to that on (▼) H_2SO_4.

initially and the average amount formed during the initial reaction period [11]. Fig. 4 reveals that the heterogeneous catalyst SAC-13 and the homogeneous catalyst H_2SO_4 exhibit very similar responses to water deactivation. Using the Arrhenius relationship, apparent activation energies were determined at initial water concentrations of 0 and 2.85 M for both catalysts (Fig. 5). Results are given in Table 2. The liquid and solid acid catalysts showed almost identical apparent reaction energy barriers at each $C_{W,0}$, with greater values at the higher initial water concentration.

4. Discussion

Thanks to the strong electron-withdrawing α-CF_2-polymer moiety, the Nafion resin is known to have a similar acid strength to H_2SO_4, as estimated by Hammett H_0 values ($-H_0 \sim 12$) [10]. Taking into account the almost unrestricted site accessibility of the highly-dispersed nano-Nafion domains on the porous silica matrix in SAC-13, the smaller intrinsic activity shown by the heterogeneous catalyst may be due to the in-

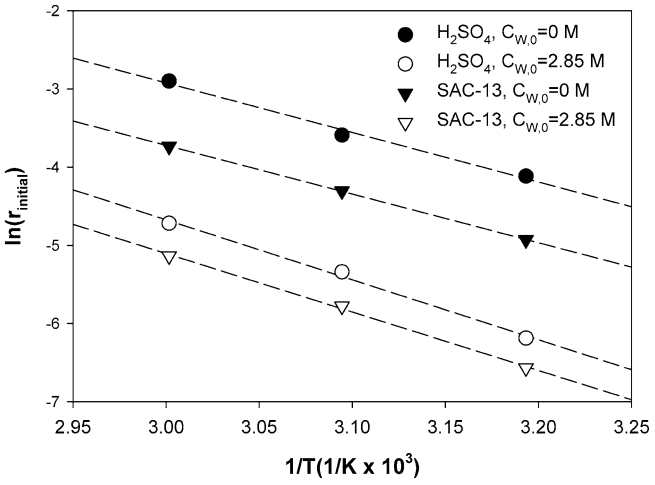

Fig. 5. Arrhenius plots for acetic acid esterification at different initial water concentrations using (●, ○) H_2SO_4 and (▼, ▽) SAC-13 ($T = 40$–$60\,^{\circ}C$, $C_{M,0}/C_{A,0} = 2$).

teraction of the polymer with the silanol groups of the silica support, resulting in decreased activity of the sulfonic acid group [20]. Alternatively, the lower observed site activity of SAC-13 might be due to the more restricted conformation of intermediate complexes adsorbed on the solid surface compared with those moving freely in solution. A reduction in the number of available energy levels of the transition state could give rise to a lower pre-exponential factor (or activation entropy in terms of "transition state theory") [21]. Nevertheless, the apparent activation energy determined for the heterogeneous acid catalyzed esterification is essentially identical to that for homogeneous catalysis (Fig. 5, Table 2), pointing to the possibility of the same rate-limiting step involved in SAC-13- and H_2SO_4-catalyzed esterification.

One more similarity between H_2SO_4- and SAC-13-catalyzed esterification of acetic acid with methanol is the positive dependency of reaction rate on the concentrations of both reagents (Table 3). Our experimental data agree with those obtained by Altiokka and Citak [8] for the esterification of acetic acid and isobutanol catalyzed by Amberlite resins at 60 °C. In contrast, Nijhuis et al. [7] reported that the SAC-13-catalyzed esterification of hexanoic acid in cumene at 150 °C decreased with increasing concentration of *n*-octanol. Studies in our group of the gas-phase esterification of acetic acid with methanol catalyzed by SAC-13 at 100–120 °C have also shown a negative reaction order for methanol [22]. These seemingly contradictory results, however, can be understood assuming a mechanistic pathway operating in a way similar to the accepted homogeneous mechanism for esterification. We discuss this in more detail later.

The effect of water on activity allows for a means to compare the similarities and differences between homogeneous and heterogeneous catalysis mechanisms. The solid and liquid acid catalysts had the same water deactivation profile (Fig. 4), suggesting that water deactivates the active sites of the solid and liquid catalysts in probably the same way, and that the mechanistic route involved in SAC-13 esterification catalysis resembles that of H_2SO_4.

One might expect water deactivation of SAC-13 and of H_2SO_4 to be similar, because both have Brønsted-type acid sites for catalysis. Even though silica contains silanol groups, their contribution to acid catalysis should be negligible because of their low acid strength [23]. We have found, for instance, that sodium-exchanged SAC-13 presents no activity for HAc esterification at 60 °C. Using pure silica, Samantaray and Parida [24] found negligible activity for the esterification of acetic acid with butanol, as did Wang et al. [25] for transesterification of dimethyl oxalate with phenol and Mbaraka et al. for esterification of palmitic acid with methanol [26]. Consequently, the $–CF_2–SO_3H$ group in SAC-13 must be fully responsible for the catalytic activity. It, like $HO–SO_3H$ (H_2SO_4), would be susceptible to solvation and proton transfer [27]. The common nature of the acid sites of both catalysts constitutes probably the most important basis for the similar water sensitivities of SAC-13 and H_2SO_4. Although the Brønsted acid sites are anchored to a solid surface in SAC-13, in condensed media containing polar molecules, these sites can still be solvated, giving rise to hydrogen-bonded clusters of polar molecules around them with proton-transfer ability [28]. In fact, the IR spectrum of hydrated Nafion-H has been reported to resemble that of an aqueous solution of concentrated H_2SO_4 [29]. Hybrid inorganic–organic silicas with immobilized sulfonic groups have also been found to behave in water essentially like homogeneous-phase p-toluenesulfonic acid (p-TsOH) [30]. In our previous study of the esterification of acetic acid with methanol catalyzed by H_2SO_4, water deactivated the catalyst by decreasing its acid strength [11]. It was suggested that the deactivating effect of water was due to the preference for water solvation of the protons over methanol solvation. The driving force behind this behavior was probably water's better ability to form hydrogen-bonding networks that can delocalize "free" protons in solution [11]. Similar reports of loss of acid strength with the addition of water have been made for Nafion-H. Buzzoni et al. [29] reported a higher red shift for O–H stretching frequencies of Nafion-H contacted with water than for methanol-contacted Nafion-H, indicating a lower acidic character for the water-solvated resin. Using acid–base calorimetric titration, Koujout and Brown [30] demonstrated how the acid strengths of sulfonic acid silicas and p-TsOH (p-toluenesulfonic acid) were influenced by their chemical surroundings. These authors were able to show a clear trend of decreasing acid strength as the solvent varied from cyclobenzene to acetonitrile to water.

Despite all evidence pointing to water having a similar inhibiting effect on esterification for SAC-13 as it does for H_2SO_4, SAC-13 did exhibit slightly less deactivation by water than H_2SO_4 at high water concentrations (Fig. 4). This observation supports the view of Nusterer et al. [31] that water solvation of solid acid sites is sterically hindered by the support matrix compared with solvation of free protons in the liquid phase. In addition, thermochemical comparisons of homogeneous p-TsOH and heterogeneous acid resin (Dowex 50W-X8) by Arnett et al. [13] showed that the liquid acid underwent a more significant decay in the heat of ionization of pyridine ($-\Delta H_i$) with increasing water concentration than the solid acid resin (Table VII and Fig. 3 in [13]). A loss of 13.6 kcal/mol

in $-\Delta H_i$ was determined for the former as the water/acid ratio increased from 0 to 10.3, whereas a loss of only 8.7 kcal/mol was found for the latter as the water/acid ratio increased from 0 to 11.4 [13]. However, this large difference in $-\Delta H_i$ may not properly reflect the actual difference in acid strength variation due to water solvation for solid and liquid acid catalysts. Given the significant swelling effect of water on Dowex 50W-X8, which could expose a greater number of acid sites, the loss of acid strength may be compensated for in part. For instance, acetic acid esterification catalyzed by SAC-13 shows only a slightly lower increase in the energy barrier in the presence of water than does that catalyzed by H_2SO_4, 10.4 versus 11.1 kJ/mol (Fig. 5, Table 2). It should be noted, however, that the apparent activation energy determined in this work for H_2SO_4 catalysis with THF as the solvent is about 7 kJ/mol greater than that reported in previous work [11] in which no solvent was used. This difference suggests that changes in the polarity of the media due to the solvent THF (vs only methanol) may affect the reaction. Nonetheless, this effect is minor compared to that of water, given the large quantity of solvent used.

To explore whether the molecular pathway for esterification on SAC-13 resembles that of H_2SO_4 (which is single site), a series of pyridine poisoning experiments were conducted to determine whether the reaction followed a single-site or a dual-site mechanism. Before each run, the catalyst was first immersed in a mixture of methanol-THF containing a known amount of pyridine. This immersion lasted overnight to allow complete equilibrated adsorption of the organic base on the acid sites of the catalyst. Afterward, the reactor was heated to 50 °C (methanol and THF form an azeotrope at 60 °C), and then preheated HAc was charged into the reactor to initiate the reaction. As shown in Fig. 6, the initial reaction rates decreased linearly with increasing amounts of pyridine, suggesting that the heterogeneous reaction involves a single-site mechanism. Moreover, if mono-molecular adsorption of pyridine per acid site is assumed, the acid site density of SAC-13 can be estimated by extrapolating to zero the esterification rate as a function of the pyridine concentration. The acid site density calculated in this way was 0.148 mmol/g after subtraction of the 10% adsorption of pyridine on the silanol groups of the silica surface. Although somewhat higher, this value agrees fairly well with the values obtained earlier (0.129 mmol/g) from elemental sulfur analysis and pyridine adsorption experiments, thus indicating that the reaction has complete accessibility to SAC-13 acid sites. The incomplete protonation of the organic base [14] may account for the slight overestimation. Nevertheless, the equilibrium constant for the protonation of pyridine is $>2 \times 10^4$ as estimated from reaction data (Fig. 6), following the method given by Kogelbauer et al. [14] and using an acid site density of 0.131 mmol/g for SAC-13. Clearly, this large value indicates a very strong acid–base interaction between surface sulfonic acid groups and pyridine and thus an almost complete protonation.

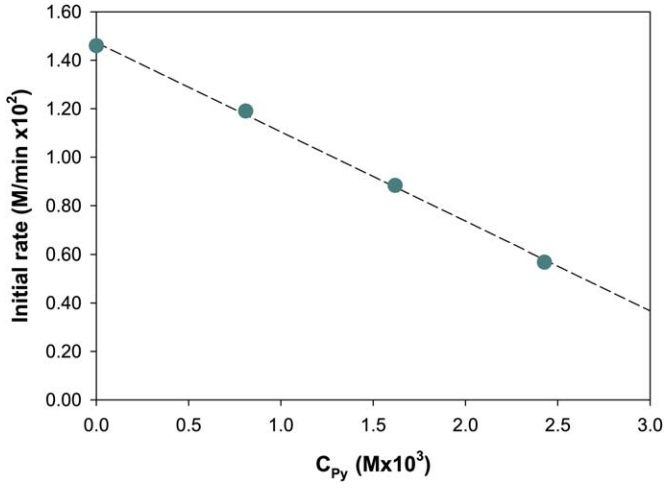

Fig. 6. Pyridine poisoning of SAC-13 catalyzed esterification of acetic acid with methanol at 50 °C ($C_{A,0} = 3$ M, $C_{M,0} = 6$ M, C_{Py} = concentration of pyridine).

The existing strong correlations in observed esterification kinetics between SAC-13 and H_2SO_4 point to similar mechanistic pathways. Thus, the evidence in terms of site activity, apparent activation energy, water deactivation behavior, and single-site mechanism strongly suggests that SAC-13-catalyzed esterification likely proceeds via a mechanism analogous to the homogeneous catalyzed one,

$$\mathrm{M} + \mathrm{S} \overset{k_1}{\rightleftarrows} \mathrm{M \cdot S}, \tag{M.1}$$

$$\mathrm{A} + \mathrm{S} \overset{k_2}{\rightleftarrows} \mathrm{A \cdot S}, \tag{M.2}$$

$$\mathrm{A \cdot S} + \mathrm{M} \overset{k_3}{\rightleftarrows} \mathrm{E \cdot S} + \mathrm{W}, \tag{M.3}$$

$$\mathrm{E \cdot S} \overset{k_4}{\rightleftarrows} \mathrm{E} + \mathrm{S}, \tag{M.4}$$

$$\mathrm{W} + \mathrm{S} \overset{k_5}{\rightleftarrows} \mathrm{W \cdot S}, \tag{M.5}$$

where M represents methanol, S is a vacant acid site on the catalyst surface, A is acetic acid, E is methyl acetate, and W is water. M · S, A · S, E · S, and W · S are molecules adsorbed on the catalytic acid sites, respectively. In the above mechanism, (M.2)–(M.4) in order depict the activation of carbonyl oxygen of acetic acid, the nucleophilic attack of protonated acetic acid by methanol forming ester and water, and the deprotonation of methyl acetate. Because methanol is a strong nucleophile, it also competes for the catalyst acid sites with acetic acid, as does water once it is produced from reaction, as shown in (M.1) and (M.5), respectively.

Let us first consider what occurs during the initial reaction period when reverse hydrolysis is not important. Using the pseudo-steady-state approximation for the protonated complexes (M · S and A · S) and solving for $C_{A\cdot S}$ with the site balance ($\rho \cdot C_C = C_{A\cdot S} + C_{M\cdot S} + C_S$) gives the rate expression

$$r = \frac{k_2 k_3 \rho C_C C_M C_A}{(k_{-2} + k_3 C_M)\left(1 + K_M C_M + \frac{k_2}{k_{-2}+k_3 C_M} C_A\right)}, \tag{1}$$

where C_C, C_M, and C_A are the concentrations of catalyst, methanol, and acetic acid, respectively; ρ denotes the site density of the catalyst; K_M represents the adsorption equilibrium constant for methanol on the Brønsted acid sites; k_2 and k_{-2}

are the acetic acid adsorption and desorption constants, respectively; and k_3 is the surface reaction constant.

If the surface reaction (k_3) is favored over the adsorption and desorption of the acid (k_2 and k_{-2}), $k_3 C_M \gg k_2, k_{-2}$, then Eq. (1) can be approximated by

$$r = \frac{k_2 \rho C_C C_A}{1 + K_M C_M}. \tag{2}$$

If, on the other hand, the opposite is true with the adsorption and desorption process being faster than surface reaction, $k_3 C_M \ll k_2, k_{-2}$, then Eq. (1) reduces to

$$r = \frac{k_2 k_3 \rho C_C C_M C_A}{k_{-2}\left(1 + K_M C_M + \frac{k_2}{k_{-2}} C_A\right)}. \tag{3}$$

Defining $K_A = k_2/k_{-2}$ as the adsorption equilibrium constant of the carboxylic acid, we have

$$r = \frac{(K_A k_3 \rho) C_C C_M C_A}{1 + K_M C_M + K_A C_A} = \frac{k C_C C_M C_A}{1 + K_M C_M + K_A C_A}, \tag{4}$$

where k is a lumped constant equivalent to $K_A k_3 \rho$. Note that although surface reaction, (M.3), occurs by an E-R mechanism, Eq. (4) is not a typical E-R rate expression due to the competing adsorption of methanol on acid sites.

From the standpoint of the two extreme situations give above, inconsistencies among reports studying acid-catalyzed esterifications using solid Brønsted acid-catalysts can be explained by a shift in the terms dominating the reaction kinetic behavior. If, for instance, as the temperature is raised, the kinetic behavior characterized by Eq. (4) evolves into behavior characterized by Eq. (2), then one would expect that after a certain point the reaction order of methanol would transit from positive to negative. This may explain what has been reported earlier for heterogeneous acid-catalyzed esterification at 100 °C and above [7,22]. Under the conditions used in this study, however, the positive reaction order determined for methanol suggests that Eq. (4) should apply.

Nonetheless, to further confirm our hypothesis ($k_3 C_M \ll k_2, k_{-2}$) for the reaction at 60 °C, experiments using catalyst samples presaturated with HAc before initiating the reaction by charging preheated methanol were carried out (results not shown). The logic behind these experiments was that if the adsorption/desorption of acetic acid was comparable to or slower than the surface reaction, then an initial reaction rate different from that obtained when the catalyst was added last (no preadsorbed HAc) would be obtained given that acetic acid was already adsorbed on the catalyst surface ready for attack by methanol. In particular, in a parallel study of the gas-phase esterification of HAc with methanol on SAC-13 at 100 °C, experiments in our laboratory using the preadsorption of HAc showed faster initial reaction rates, indicating that under these conditions, the surface reaction of acetic acid was not the rate-controlling step [22]. However, the results for liquid-phase esterification at 60 °C showed no improvement in the initial reaction rates compared with experiments using the catalyst with no preadsorbed carboxylic acid. Hence, rapid reagent adsorption/desorption equilibrium with surface reaction as the rate-limiting step is likely the case under our reaction conditions, appearing to further confirm Eq. (4) as the suitable kinetic model.

Using Eq. (4) and initial reaction rate (r_0) measured at various initial reactant compositions, a mathematical model was developed to predict esterification rate as reaction progresses. Equation (4) can be rearranged to give

$$\frac{1}{r_0} = \frac{K_M}{k C_C C_{A,0}} + \frac{1 + K_A C_{A,0}}{k C_C C_{A,0}} \left(\frac{1}{C_{M,0}}\right) \tag{5}$$

or

$$\frac{1}{r_0} = \frac{K_A}{k C_C C_{M,0}} + \frac{1 + K_M C_{M,0}}{k C_C C_{M,0}} \left(\frac{1}{C_{A,0}}\right). \tag{6}$$

According to Eq. (5), when $C_{A,0}$ is fixed at 2.0 M, a plot of $1/r_0$ versus $1/C_{M,0}$ yields a straight line with the ratio slope/intercept equal to $(1 + 2K_A)/K_M$. Likewise, $(2K_M + 1)/K_A$ can be determined from the plot of $1/r_0$ versus $1/C_{A,0}$. The plots based on Eqs. (5) and (6) are shown in Figs. 7a and 7b, respectively. In this way, K_M and K_A were calculated as 0.16 and 0.13 L/mol, respectively. The somewhat larger adsorption equilibrium constant for methanol compared with acetic acid is consistent with its lower apparent reaction order, indicating more extensive methanol coverage of the acid sites.

As was determined earlier, water can seriously inhibit SAC-13 catalysis (Fig. 5). Therefore, as water is continuously produced by the reaction, the adsorption term of water must be included in the kinetic expression. For initial kinetics measurements in the presence of added water, Eq. (4) should then be

$$r_0 = \frac{k C_C C_{M,0} C_{A,0}}{1 + K_M C_{M,0} + K_A C_{A,0} + K_W C_W}. \tag{7}$$

Rearranging this equation, we get

$$\frac{1}{r_0} = \frac{1 + K_M C_{M,0} + K_A C_{A,0}}{k C_C C_{M,0} C_{A,0}} + \frac{K_W}{k C_C C_{M,0} C_{A,0}} (C_W). \tag{8}$$

Using the K_A and K_M values determined previously and fixing $C_{A,0}$ (3 M) and $C_{M,0}$ (6 M), the adsorption constant for water was obtained from plots of $1/r$ versus C_W (Fig. 7c) as 3.11 L/mol.

Furthermore, an expression for k can be derived from Eq. (8) as

$$k = \frac{r_0 (1 + K_M C_{M,0} + K_A C_{A,0} + K_W C_W)}{C_C C_{M,0} C_{A,0}}. \tag{9}$$

By inserting calculated adsorption constants into Eq. (9) and using the initial kinetic data, the lumped reaction constant for acetic acid was determined to be 1.50×10^{-4} L^2/(g cat mol min). Thus far, because the adsorption of solvent and ester are known to be negligible [7,8], Eq. (7) can be expanded to include reverse reaction at high conversions,

$$-\frac{dC_A}{dt} = \frac{k C_C}{1 + K_M C_M + K_A C_A + K_W C_W} \left(C_M C_A - \frac{C_W C_E}{K_e}\right), \tag{10}$$

where K_e is the equilibrium constant for esterification ($K_e = 6.2$ at 60 °C). For a molar ratio of $C_{M,0}/C_{A,0} = n$ and an initial water addition of $C_{W,0}/C_{A,0} = u$, Eq. (10) expressed in terms of acetic acid conversion becomes

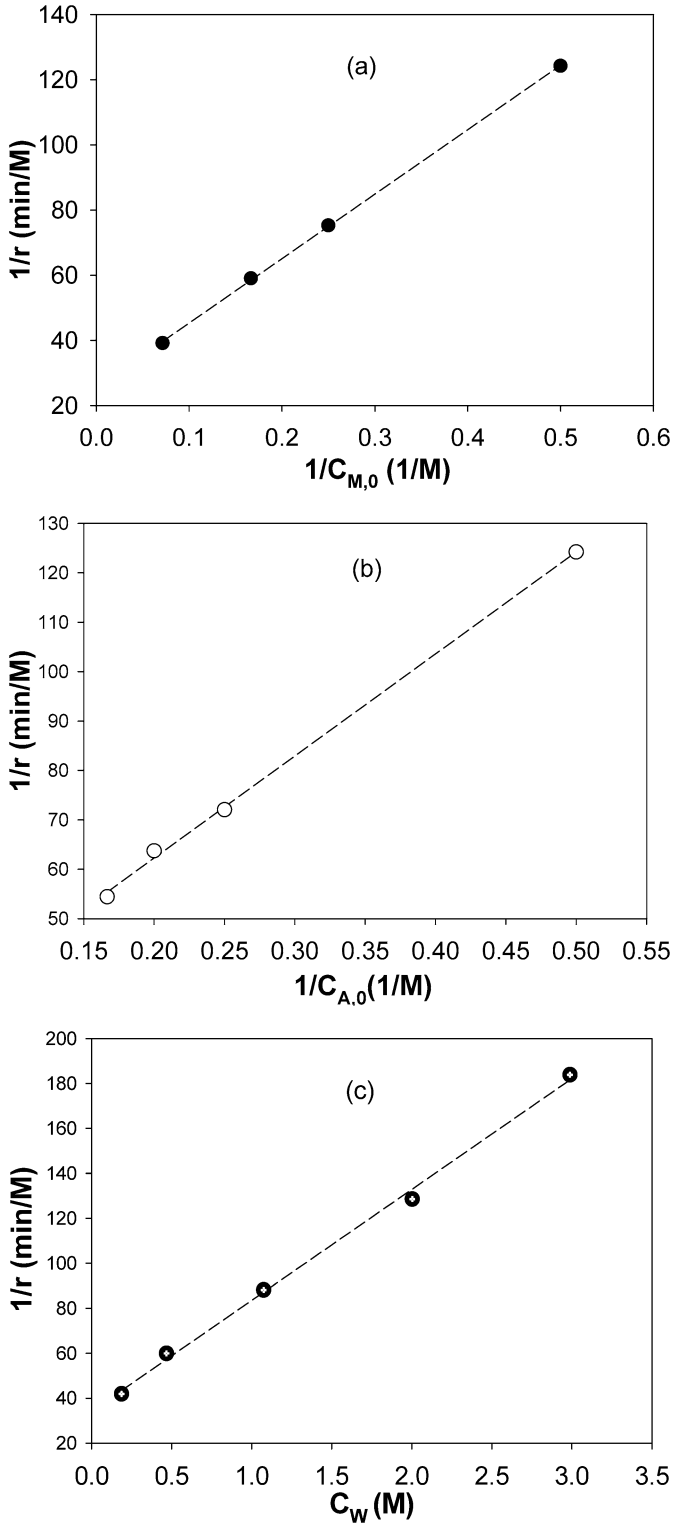

Fig. 7. Determination of the adsorption constants for (a) methanol, (b) acetic acid, and (c) water at 60 °C for SAC-13.

$$\frac{dx_A}{dt} = \frac{kC_C C_{A,0}}{1 + C_{A,0}[K_M(n - x_A) + K_A(1 - x_A) + K_W(x_A + u)]} \times \left[(n - x_A)(1 - x_A) - \frac{(x_A + u)x_A}{K_e}\right]. \quad (11)$$

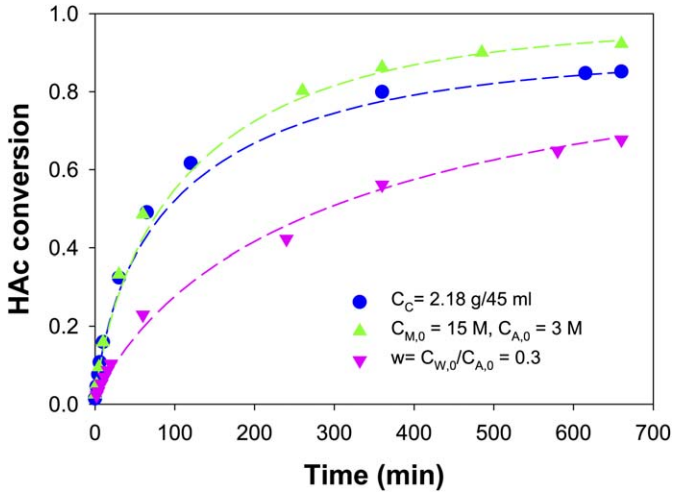

Fig. 8. Comparison of experimental data with values predicted by Eq. (11) for the esterification of acetic acid with methanol on SAC-13 under different reaction conditions (symbols represent the experimental data; dashed lines represent the model predictions).

Using numerical integration (Runga–Kutta), carboxylic acid conversion at a given time can be predicted from Eq. (11). The dotted line in Fig. 2 gives the prediction of reaction conversion based on Eq. (11). Thus, Eq. (11) satisfactorily represents the esterification of acetic acid with methanol on SAC-13.

As shown in Fig. 8, the mathematical model thus derived successfully predicts reaction profiles for the esterification of HAc using different reaction conditions from those used originally to calculate it (i.e., double loading of catalysts and higher methanol/HAc molar ratio). In addition, Fig. 8 shows how the model can accurately assess reaction profiles for esterification in the presence of initial amounts of water, supporting the estimated effect of water inhibition on SAC-13 catalysis.

5. Conclusion

The catalytic performance of the Nafion/silica nanocomposite SAC-13 was evaluated for the esterification of acetic acid with methanol and compared with that of H_2SO_4. TOF values calculated for SAC-13 showed that the activity of the resin is comparable to that of H_2SO_4 on a per site basis. It was also determined that most acid sites on the Nafion nanodomains were available for reaction without the need for polymer swelling. SAC-13 and H_2SO_4 showed similar reaction inhibition by water, suggesting a common reaction mode on their Brønsted acid sites. A typical E-R-type heterogeneous reaction mechanism involving a nucleophilic attack between adsorbed carboxylic acid and unadsorbed alcohol as the rate-limiting step closely fits the experimental data obtained under our reaction conditions. A mathematical model was analytically derived, from which it was possible to reproduce the kinetic profiles of acetic acid esterification under different experimental conditions.

References

[1] G.D. Yadav, P.H. Mehta, Ind. Eng. Chem. Res. 33 (1994) 2198.

[2] E. Lotero, Y.J. Liu, D.E. Lopez, K. Suwannakarn, D.A. Bruce, J.G. Goodwin Jr., Ind. Eng. Chem. Res. 44 (2005) 5353.
[3] R. Ronnback, T. Salmi, A. Vuori, H. Haario, J. Lehtonen, A. Sundqvist, E. Tirronen, Chem. Eng. Sci. 52 (1997) 3369.
[4] R. Koster, B. van der Linden, E. Poels, A. Bliek, J. Catal. 204 (2001) 333.
[5] H.T.R. Teo, B. Saha, J. Catal. 228 (2004) 174.
[6] M.J. Lee, H.T. Wu, H.M. Lin, Ind. Eng. Chem. Res. 39 (2000) 4094.
[7] T.A. Nijhuis, A.E.W. Beers, F. Kapteijn, J.A. Moulijn, Chem. Eng. Sci. 57 (2002) 1627.
[8] M.R. Altiokka, A. Citak, Appl. Catal. A 239 (2003) 141.
[9] J. Lilja, D.Y. Murzin, T. Salmi, J. Aumo, P.M. Arvela, M. Sundell, J. Mol. Catal. A 182 (2002) 555.
[10] M.A. Harmer, W.E. Farneth, Q. Sun, J. Am. Chem. Soc. 118 (1996) 7708.
[11] Y.J. Liu, E. Lotero, J.G. Goodwin Jr., J. Mol. Catal. A 245 (2005) 132.
[12] Q. Sun, W.E. Farneth, M.A. Harmer, J. Catal. 164 (1996) 62.
[13] E.M. Arnett, R.A. Haaksma, B. Chawla, M.H. Healy, J. Am. Chem. Soc. 108 (1986) 4888.
[14] A. Kogelbauer, J. Reddick, D. Farcasiu, J. Mol. Catal. A Chem. 103 (1995) 31.
[15] F. Omota, A.C. Dimian, A. Bliek, Chem. Eng. Sci. 58 (2003) 3175.
[16] H. Wang, B.Q. Xu, Appl. Catal. A 275 (2004) 247.
[17] P. Nowak, React. Kinet. Catal. Lett. 66 (1999) 375.
[18] X. Chen, Z. Xu, T. Okuhara, Appl. Catal. A 180 (1999) 261.
[19] A. Corma, H. Garcia, Catal. Today 38 (1997) 257.
[20] P. Botella, A. Corma, J.M. Lopez-Nieto, J. Catal. 185 (1999) 371.
[21] N.B. Chapman, M.G. Rodgers, J. Shorter, J. Chem. Soc. B (1968) 157.
[22] K. Suwannakarn, J.G. Goodwin Jr., E. Lotero, D.A. Bruce (2006), in preparation.
[23] B. Torok, I. Kiricsi, A. Molnar, G.A. Olah, J. Catal. 193 (2000) 132.
[24] S.K. Samantaray, K. Parida, React. Kinet. Catal. Lett. 78 (2003) 381.
[25] S.P. Wang, X.B. Ma, H.L. Guo, J.L. Gong, X. Yang, G.H. Xu, J. Mol. Catal. A 214 (2004) 273.
[26] I.K. Mbaraka, D.R. Radu, V.S.Y. Lin, B.H. Shanks, J. Catal. 219 (2003) 329.
[27] Y. Zimmermann, S. Spange, J. Phys. Chem. B 106 (2002) 12,524.
[28] M. Krossner, J. Sauer, J. Phys. Chem. 100 (1996) 6199.
[29] R. Buzzoni, S. Bordiga, G. Ricchiardi, G. Spoto, A. Zecchina, J. Phys. Chem. 99 (1995) 11,937.
[30] S. Koujout, D.R. Brown, Catal. Lett. 98 (2004) 195.
[31] E. Nusterer, P.E. Blochl, K. Schwarz, Chem. Phys. Lett. 253 (1996) 448.